Journal of Experimental Botany, Vol. 70, No. 3 pp. 995–1004, 2019
doi:10.1093/jxb/ery403 Advance Access Publication 4 December 2018
This paper is available online free of all access charges (see https://academic.oup.com/jxb/pages/openaccess for further details)

RESEARCH PAPER

A single serine to alanine substitution decreases bicarbonate affinity of phospho*enol*pyruvate carboxylase in C_4 *Flaveria trinervia*

Robert J. DiMario and Asaph B. Cousins*

School of Biological Sciences, Washington State University, Pullman, WA 99164, USA

* Correspondence: acousins@wsu.edu

Received 14 August 2018; Editorial decision 8 November 2018; Accepted 20 November 2018

Editor: Christine Raines, University of Essex, UK

Abstract

Phospho*enol*pyruvate (PEP) carboxylase (PEPc) catalyzes the first committed step of C_4 photosynthesis generating oxaloacetate from bicarbonate (HCO_3^-) and PEP. It is hypothesized that PEPc affinity for HCO_3^- has undergone selective pressure for a lower K_{HCO3} (K_m for HCO_3^-) to increase the carbon flux entering the C_4 cycle, particularly during conditions that limit CO_2 availability. However, the decrease in K_{HCO3} has been hypothesized to cause an unavoidable increase in K_{PEP} (K_m for PEP). Therefore, the amino acid residue S774 in the C_4 enzyme, which has been shown to increase K_{PEP}, should lead to a decrease in K_{HCO3}. Several studies reported the effect S774 has on K_{PEP}; however, the influence of this amino acid substitution on K_{HCO3} has not been tested. To test these hypotheses, membrane-inlet mass spectrometry (MIMS) was used to measure the K_{HCO3} of the photosynthetic PEPc from the C_4 *Flaveria trinervia* and the non-photosynthetic PEPc from the C_3 *F. pringlei*. The cDNAs for these enzymes were overexpressed and purified from the PEPc-less *PCR1 Escherichia coli* strain. Our work in comparison with previous reports suggests that K_{HCO3} and K_{PEP} are linked by specific amino acids, such as S774; however, these kinetic parameters respond differently to the tested allosteric regulators, malate and glucose-6-phosphate.

Keywords: Bicarbonate kinetics, C_4 photosynthesis, membrane-inlet mass spectrometery, phospho*enol*pyruvate carboxylase.

Introduction

Phospho*enol*pyruvate (PEP) carboxylase (PEPc) catalyzes the irreversible carboxylation of PEP using bicarbonate (HCO_3^-) to form the four-carbon sugar, oxaloacetate (OAA). In plants, this reaction generally influences stomatal conductance (Parvathi and Raghavendra, 1997; Cousins *et al.*, 2007), seed development (Sangwan *et al.*, 1992; O'Leary *et al.*, 2011), pH regulation (Davies, 1986; Britto and Kronzucker, 2005), and the balance between carbon and nitrogen metabolism by providing intermediates for the tricarboxylic acid (TCA) cycle (Rademacher *et al.*, 2002; Plaxton and Podestá, 2006). In mesophyll cells of C_4 plants, PEPc catalyzes the first committed step of C_4 photosynthesis by providing OAA that is subsequently modified to other four-carbon compounds before entering bundle sheath cells for decarboxylation, releasing CO_2 at the site of Rubisco (Hatch *et al.*, 1975; von Caemmerer and Furbank, 2003).

Higher plants contain multiple PEPc-encoding (*ppc*) genes comprising a multigene family where most of the

Abbreviations: CA, carbonic anhydrase; C_i, inorganic carbon; C_m, mesophyll CO_2 concentration; G6-P, glucose 6-phosphate; h, Hill value; HCO_3^-, bicarbonate; K_{HCO3}, K_m for HCO_3^-; K_{PEP}, K_m for PEP; MIMS, membrane-inlet mass spectrometry; OAA, oxaloacetate; PEG, polyethylene glycol; PEP, phospho*enol*pyruvate; PEPc, phospho*enol*pyruvate carboxylase; PTM, post-translational modification; V_P, PEPc activity; V_{Pmax}, maximum rate of PEPc carboxylation; $V_{Pmax(plant)}$, maximum rate of PEPc carboxylation per unit leaf area.

© The Author(s) 2018. Published by Oxford University Press on behalf of the Society for Experimental Biology.

This is an Open Access article distributed under the terms of the Creative Commons Attribution License (http://creativecommons.org/licenses/by/4.0/), which permits unrestricted reuse, distribution, and reproduction in any medium, provided the original work is properly cited.

genes encode a non-photosynthetic C_3 PEPc (Christin and Besnard, 2009). C_4 plants obtained a modified PEPc isoform to power C_4 photosynthesis through mutations to a native *ppc* coding region (Christin *et al.*, 2007; Rosnow *et al.*, 2014) and upstream promoter region (Schaffner and Sheen, 1992; Gowik *et al.*, 2004). Changes to the C_4 *ppc* promoter region led to strong, mesophyll-specific expression, resulting in high PEPc activity to drive the CO_2-concentrating mechanism of C_4 photosynthesis (Gowik *et al.*, 2004). Work on PEPc peptide sequences from members of the Poaceae, Amaranthaceae, Asteraceae, and Cyperaceae families (Christin *et al.*, 2007), as well as the Chenopodaceae family (Rosnow *et al.*, 2014), identified amino acid residues predicted to be under positive selection in these C_4 lineages. Comparing PEPc sequences of species within and between families shows that C_4 PEPc isoforms from different species possess different combinations of amino acid residues under positive selection (Christin *et al.*, 2007; Rosnow *et al.*, 2014). These findings suggest that there are multiple ways the C_4 PEPc kinetic properties can arise in different C_4 origins or that there is diversity in the PEPc kinetics between species.

An increase in PEPc activity in the leaf mesophyll cytosol in the intermediate C_3/C_4 species would be likely to lead to selection for changes in kinetic properties (Westhoff and Gowik, 2004). This was previously tested in a variety of C_3/C_4 species that displayed a progression in altered K_{PEP} (K_m for PEP) and decreased malate sensitivity (Westhoff and Gowik, 2004). C_4 plants contain high levels of malate in the mesophyll cytosol, so there would be selection for amino acid substitutions that transition the malate-sensitive C_3 PEPc to a less sensitive C_4 PEPc (Bläsing *et al.*, 2002; Paulus *et al.*, 2013). This is supported by the Gly884 substitution in the *Flaveria trinervia* C_4 PEPc to the *Flaveria pringlei* C_3 PEPc arginine that caused the C_4 PEPc to lose its resistance to malate (Paulus *et al.*, 2013).

As PEPc transitioned from C_3 to C_4 function, it has been suggested that certain amino acid substitutions were under positive selection to alter K_{PEP} and K_{HCO3} (K_m for HCO_3^-). It is hypothesized that certain mutations in the C_4 *ppc* coding region resulted from strong selective pressures to obtain a lower K_{HCO3} than that of the C_3 PEPc (Jacobs *et al.*, 2008). The lower K_{HCO3} of the C_4 PEPc may enhance the efficiency of C_4 photosynthesis, especially when HCO_3^- availably is low due to reduced stomatal conductance. Alternatively, the C_4 PEPc has been shown to have a higher K_{PEP}, with values typically reported between 100 μM and 590 μM (Svensson *et al.*, 1997; Dong *et al.*, 1998; Westhoff and Gowik, 2004; Lara *et al.*, 2006; Rosnow *et al.*, 2015), as compared with C_3 non-photosynthetic PEPc K_{PEP} values which range from 13 μM to 60 μM (Westhoff *et al.*, 1997; Bläsing *et al.*, 2002; Gowik *et al.*, 2006; Lara *et al.*, 2006; Rosnow *et al.*, 2015). It was hypothesized that this increase in C_4 K_{PEP} was an unavoidable consequence of the reduction of K_{HCO3} since the two kinetic traits may be linked by certain amino acids (Jacobs *et al.*, 2008; Gowik and Westhoff, 2011). Alternatively, since the PEP pools in a C_4 leaf are higher than in a C_3 leaf, the high K_{PEP} of the C_4 PEPc may ensure stronger diurnal regulation of PEPc (Budde and Chollet, 1986; Hatch, 1987).

Residue S774 in *F. trinervia* (S780 in maize) was shown to be under positive selection by Poetsch *et al.* (1991) and Hermans and Westhoff (1992), and substituting the conserved C_4 serine for the conserved C_3 alanine in *F. trinervia* (S774A) significantly decreased the K_{PEP} of the C_4 PEPc (Bläsing *et al.*, 2000; Engelmann *et al.*, 2002). Since the S774A substitution affects the K_{PEP} of PEPc, it is possible that it may also affect the K_{HCO3}, making S774 one of the residues potentially linking K_{PEP} and K_{HCO3}. However, this serine residue was unimportant for the high K_{PEP} in the C_4 Chenopodaceae (Rosnow *et al.*, 2014).

The only study to publish K_{HCO3} of both a C_3 and C_4 PEPc showed that the K_{HCO3} of five C_4 species representing the Poaceae and Amaranthaceae families was ~26 μM compared with preliminary evidence suggesting that the K_{HCO3} of the C_3 PEPc from *Flaveria cronquistii* (Asteraceae family) was 80 μM (Bauwe, 1986). Other studies reported C_4 PEPc K_{HCO3} values ranging from 14 μM to 180 μM (Janc *et al.*, 1992; Gao and Woo, 1995; Parvathi *et al.*, 2000; Boyd *et al.*, 2015), where the C_3 K_{HCO3} of 80 μM falls within this reported range of C_4 K_{HCO3} values. However, comparing K_{HCO3} for closely related C_3 and C_4 PEPc isoforms can provide a more accurate analysis of the change in C_3 to C_4 K_{HCO3} and whether there was a strong selective force on PEPc K_{HCO3}, but to date this has not been performed. Additionally, the previously reported K_{HCO3} values were obtained by coupling PEPc activity to spectrophotometrically measured NADH oxidation rates. It is difficult to obtain accurate K_{HCO3} values using this method because it does not directly measure changes in HCO_3^- concentration in the assay. This is problematic because measurements of K_{HCO3} require accurate determinations of PEPc activity and HCO_3^- concentrations below the K_{HCO3}, which is in the micromolar range. To overcome this problem, membrane-inlet mass spectrometry (MIMS) can be used to measure HCO_3^- consumption by PEPc accurately and directly in real-time over a wide range of inorganic carbon (C_i) concentrations, including concentrations well below the K_{HCO3}, without the complication of coupling PEPc activity to the NADH dehydrogenase reaction (Boyd *et al.*, 2015).

In this study, we use MIMS to obtain K_{HCO3} values for the photosynthetic PEPc from the C_4 plant *F. trinervia* and the non-photosynthetic PEPc from the C_3 plant *F. pringlei* that were overexpressed and purified from the PEPc-less *PCR1 Escherichia coli* strain (Sabe *et al.*, 1984; Svensson *et al.*, 1997). We found that the S774A substitution increases the C_4 K_{HCO3}, whereas the A774S substitution did not affect the C_3 K_{HCO3}, suggesting that additional amino acids besides S774 are involved in the C_4 K_{HCO3} trait. Since previous studies reported PEPc K_{PEP} changing in the presence of the allosteric activator glucose 6-phosphate (G6-P) and the inhibitor malate (Huber and Edwards, 1975; Wedding *et al.*, 1990; Gupta *et al.*, 1994; Bläsing *et al.*, 2002), we tested whether these allosteric regulators also affected K_{HCO3}. We report that G6-P and malate have a minimal effect on the K_{HCO3} of PEPc. We address how differences in calibration methods, assay conditions, and enzyme extractions can produce different *in vitro* kinetic values, and we report an improvement to the MIMS PEPc assay. Lastly, we demonstrate how the decrease in K_{HCO3} between the C_3 and

C_4 PEPc isoforms increases the modeled rates of C_4 photosynthesis at low CO_2 concentrations.

Materials and methods

Generating PCR1 *PEPc-overexpressing lines*

The PEPc-less *E. coli* strain, *PCR1* (Sabe *et al.*, 1984), and PEPc cDNA constructs used in Svensson *et al.* (1997) and Bläsing *et al.* (2000) were generously provided by Professor Peter Westhoff's lab. The plasmid, pTrc99A, carrying the cDNA coding for either the C_4 *F. trinervia* PEPc, the C_3 *F. pringlei* PEPc, or *Flaveria* PEPc with either an alanine or serine substitution at residue 774, C_4-S774A or C_3-A774S, respectively, was transformed into the *PCR1 E. coli* strain. *PCR1* transformants producing plant PEPc were selected following the method of Svensson *et al.* (1997).

Growth of PCR1 *PEPc-overexpressing lines for PEPc extraction*

A 4 ml growth culture (Luria–Bertani broth; 0.1% w/v dextrose; 100 μg ml^{-1} ampicillin) was inoculated with a glycerol stock of the *PCR1* strain carrying a *Flaveria* PEPc construct and was incubated at 28 °C with shaking at 160 rpm overnight. The following morning, the 4 ml culture was centrifuged at 1538 *g* for 10 min at room temperature. The supernatant was discarded, and the bacterial pellets were resuspended and transferred to a large 500 ml growth culture which was incubated at 28 °C and shaken at 160 rpm. After 6 h of incubation, isopropyl-β-D-1-thiogalactopyranoside (IPTG) was added to a final concentration of 100 μM to the 500 ml growth culture to induce PEPc production overnight.

PEPc extraction and purification from E. coli

The 500 ml growth culture was centrifuged at 2602 *g* for 10 min at room temperature and the bacterial pellets were resuspended in a total volume of 20 ml of ice-cold lysis buffer [50 mM Tris–HCl, pH 8.0; 0.5 M NaCl; 10 mM DTT; 1 mM EDTA, pH 8.0; 20 μl ml^{-1} *E. coli* protease inhibitor (Sigma); 1 mg ml^{-1} lysozyme (Bioworld); 10% (v/v) glycerol; 20% (w/v) sucrose]. The resuspended cells were placed in ice for 30 min and then lysed via sonication (BioLogics Ultrasonic Homogenizer 300 V/T). The sonicated cells were transferred to centrifuge tubes and were spun at 30 597 *g* for 30 min at 4 °C. The supernatant was collected and $MgCl_2$ was added to the supernatant to a final concentration of 10 mM. Polyethylene glycol (50% PEG 8000) was added to the supernatant to a final concentration of 6% (v/v) before placing the supernatant on ice for 15 min with gentle mixing. The supernatant was again spun at 30 597 *g* for 20 min at 4 °C. The protein pellets were discarded and 50% PEG 8000 was added to the final concentration of 12% (v/v). The supernatant was slowly stirred on ice for 15 min before centrifugation at 30 597 *g* for 20 min at 4 °C.

The protein pellet was collected and resuspended in 6 ml of Buffer A [0.5 M $(NH_4)_2SO_4$; 20 mM Tris–HCl, pH 7.5; 0.1 mM DTT; 1 mM EDTA, pH 8.0; 5% (v/v) glycerol] supplemented with 1 mM phenylmethylsulfonyl fluoride (PMSF) (Svensson *et al.*, 1997). The protein sample was loaded onto a HIC phenyl–Sepharose column (1 cm×5.5 cm) pre-incubated with Buffer A at a flow rate of 1.5 ml min^{-1}. The hydrophobic properties of PEPc were used for the partial purification of PEPc by following the protocol of Svensson *et al.* (1997).

Fractions from the phenyl–Sepharose column were analyzed for PEPc activity by coupling the PEPc and NADH dehydrogenase reactions following the protocol of Boyd *et al.* (2015). Fractions displaying the highest PEPc activity were pooled and desalted in Buffer B [100 mM HEPES-KOH, pH 7.6; 1 mM DTT; 1 mM EDTA, pH 8.0] and concentrated using Corning Spin-X UF columns (6 ml volume, 100 K molecular weight cut-off) according to the Corning procedure. Glycerol was added to a final concentration of 20% (v/v) before storage at –80 °C. Total protein content of the PEPc samples was measured by a modified Bradford assay (Bio-Rad Protein Assay Kit II) (Bradford, 1976) using the Bio-Rad procedure.

Extracting PEPc from F. trinervia *and* Setaria viridis

PEPc samples were extracted and desalted from leaves of *F. trinervia* and *S. viridis* following the procedure of Boyd *et al.* (2015). Once the desalted PEPc extracts were collected and moved through a Millex-GP 0.22 μm syringe filter (Millipore), the extracts were concentrated by spinning the samples at 2880 *g* for 20 min at 4 °C in an Amicon Ultra-4 Ultracel-100K centrifugal filter (Millipore). Glycerol was added to the concentrated PEPc samples to a final concentration of 20% (v/v) and stored at –80 °C.

Obtaining V_{Pmax}, K_{HCO3}, *and Hill values for the different PEPc isoforms*

The HCO_3^--dependent PEPc assays were run in a 600 μl cuvette attached to the inlet of a mass spectrometer as described by Cousins *et al.* (2010). A CO_2 calibration was conducted before each HCO_3^- response curve as reported by Boyd *et al.* (2015). The calibration consisted of three 2 μl injections of 10 mM $NaHCO_3$ into 0.1 N HCl and three 6 μl injections of 100 mM $NaHCO_3$ into the PEPc reaction mixture [100 mM HEPES-KOH, pH 7.6; 10 mM $MgCl_2$; 1 mM DTT; 50 μg ml^{-1} carbonic anhydrase (CA); 5 mM G6-P; 5 mM PEP]. The second calibration step differs from Boyd *et al.* (2015) as their 100 mM $NaHCO_3$ injections went into buffer lacking DTT, G6-P, and PEP. DTT, G6-P, and PEP were added to the second calibration to take into account the pH changes these compounds have on the assay buffer. As the CO_2 calibrations take into account total C_i and total CO_2 in the cuvette, the HCO_3^- concentration could be deduced by subtracting the amount of CO_2 in the cuvette from the total C_i measured in the cuvette (Boyd *et al.*, 2015).

To measure PEPc HCO_3^- kinetics, seven $NaHCO_3$ concentrations (50, 100, 200, 350, 500, 750, and 1000 μM) were used for the assays. The CO_2 was removed from the assay buffer containing 100 mM HEPES-KOH, pH 7.6 and 10 mM $MgCl_2$ by continuously bubbling the buffer with humidified N_2 gas starting at least 1 h prior to initiating the assays. The assay buffer (600 μl) followed by 1 mM DTT, 50 μg ml^{-1} CA, 5 mM G6-P, 5 mM PEP, and various $NaHCO_3$ concentrations were added to the reaction cuvette and held at a constant 25 °C with a temperature-controlled water bath.

A blank rate was obtained by measuring the change in the mass 44 ($^{12}C^{16}O^{16}O$) signal during a 30 s period before initiating the reaction with the addition of 10–15 μg of total protein of the PEPc extract. The PEPc reaction was run for 5 min but the first 20 s of the PEPc reaction were discarded to allow for enzyme mixing and rate stabilization. The MIMS reports a mass 44 signal every 0.8 s, so a robust 10 s running average of the change in mass 44 was used as a single data point for PEPc activity (V_P) at an averaged [HCO_3^-]. Data points from 10 s running averages were taken immediately following the 20 s mixing phase. For the larger $NaHCO_3$ injections (350–1000 μM $NaHCO_3$), 10 s running averages were taken until a drop in PEPc activity was observed to avoid data points where there might be end-product inhibition of the reaction. For the lower $NaHCO_3$ concentrations (50–200 μM), 10 s running averages were taken until the reaction was depleted of C_i. Once the C_i was depleted from the 50, 100, and 200 μM $NaHCO_3$ injections, as indicated by a zero slope for the mass 44 signal, a 30 s running average of the zero slope was taken to obtain a mass 44 zero. These mass 44 zeroes accounted for mechanical drift in the MIMS as the different zeroes were taken at various times throughout the HCO_3^- response curve.

The kinetic parameters V_{Pmax}, K_{HCO3}, and Hill value (h) were obtained by using the Hill equation:

$$V_P = \frac{V_{Pmax} \times \left[HCO_3^-\right]^h}{\left(K_{HCO3}\right)^h + \left[HCO_3^-\right]^h} \quad (1)$$

where the Hill equation was fit to the HCO_3^- response curve using Excel's Solver function to produce the kinetic parameters listed above.

Measuring the impact of G6-P and malate on K_{HCO3}

To measure the effect of G6-P on K_{HCO3}, G6-P was omitted from the assay described above to compare K_{HCO3} values in the presence or absence of 5 mM G6-P. Alternatively, 2.5 mM malate (pH 7.6) was added to the assay described above to determine if malate affects PEPc K_{HCO3} values in the presence or absence of G6-P.

Measuring PEP effects on malate inhibition

The MIMS assay described above was used to determine if PEP concentration affects malate inhibition of PEPc, in the absence of G6-P. Five malate concentrations were used (0, 1, 2, 3, and 4 mM) to determine the percentage change in enzyme activity of the C_3 and C_4 PEPc isoforms in the presence of saturating $NaHCO_3$ (1000 µM) and when PEP was saturating (5 mM) or non-saturating (150 µM and 750 µM for the C_3 and C_4 isoforms, respectively). The non-saturating PEP concentrations were determined to be twice the reported K_{PEP} values ($2\times K_{PEP}$) in the absence of G6-P (Westhoff and Gowik, 2004).

Extraction source, pH, and calibration effects on PEPc K_{HCO3}

Previously, MIMS measurements of desalted PEPc extracts from *S. viridis* reported a K_{HCO3} of 62.8 ± 5.0 µM (Boyd *et al.*, 2015). Therefore, we tested whether differences in PEPc source (plant versus *E. coli*), pH, or MIMS calibrations caused the K_{HCO3} reported here to differ from those of Boyd *et al.* (2015). The MIMS assay described above containing 5 mM G6-P and no malate was used to test whether PEPc samples extracted from leaves of *F. trinervia* and *S. viridis* produced different K_{HCO3} values from the C_4 PEPc extracted from *E. coli*. For each assay, 5–10 µl of plant extract was added to initiate the PEPc reaction. PEPc extracts from *S. viridis* were used to compare K_{HCO3} values obtained at pH 7.6, the pH used in this study, with K_{HCO3} values obtained at pH 7.8 used by Boyd *et al.* (2015). These extracts were also used to compare K_{HCO3} values obtained at pH 7.8 using either the current calibration method outlined above or the calibration method of Boyd *et al.* (2015).

Statistical analysis of experimental data

Statistical analyses of the kinetic data were performed using RStudio version 1.1.447 (RStudio Team, 2016). Homogeneity of variance was checked using Levene tests, and normality was checked using residual quantile plots and residual versus fitted value plots. Non-normal data were log transformed but they reported the same statistical outcomes as non-transformed data, so for simplicity only non-transformed data analyses are presented. One-way ANOVA and Tukey HSD post-hoc tests were used to determine statistical significance ($P<0.05$) of K_{HCO3} between PEPc isoforms. Two-way ANOVA ($P<0.05$) and Tukey HSD post-hoc tests were used to analyze statistically significant differences in K_{HCO3} between isoforms and the impact of potential allosteric effectors. A two-way repeated measures ANOVA ($P<0.05$) was used to test if the change in PEPc activity in response to malate significantly differed between C_3 and C_4 PEPc isoforms at various PEP concentrations. One-way ANOVA and Tukey HSD post-hoc tests were used to determine significant differences between C_4 PEPc extracted from *E. coli* and PEPc extracted from *F. trinervia* and *S. viridis* leaves. Student's *t*-tests ($P<0.05$) were separately used to determine significant differences in *S. viridis* PEPc K_{HCO3} assayed at pH 7.6 and 7.8 and for *S. viridis* PEPc K_{HCO3} assayed at pH 7.8 using the two calibration methods.

Modeling the effect of K_{HCO3} on C_4 photosynthesis

The modeled effect of K_{HCO3} on the response of C_4 enzyme-limited photosynthetic CO_2 assimilation (A_c) to changing mesophyll CO_2 concentrations (C_m) was determined by solving the quadratic formula using the set of equations as described by von Caemmerer (2000). The equations and input variables were taken from von Caemmerer *et al.* (1994), von Caemmerer (2000), Tholen and Zhu (2011), and Ubierna *et al.* (2013), and are presented in Supplementary Table S1 at *JXB* online.

Results

Kinetics of the C_3, C_4, and chimeric PEPc isoforms

The Hill equation was used to determine the maximum rate of PEPc carboxylation (V_{Pmax}), the K_m for bicarbonate (K_{HCO3}), and the co-operativity of the PEPc active sites (h) from 25 °C MIMS measurements of PEPc activity (V_p) in response to changes in HCO_3^- concentrations (Supplementary Fig. S1). Measurements were made on C_4, C_3, and chimeric *Flaveria* PEPc isoforms expressed and partially purified from *E. coli*. The C_4 PEPc had a significantly lower K_{HCO3} than the C_3 PEPc, 26.6 ± 1.7 µM and 64.0 ± 2.4 µM, respectively (Fig. 1). Additionally, the C_3 PEPc had a lower V_{Pmax} compared with the C_4 PEPc, 5.1 ± 0.7 µmol mg protein^{-1} min^{-1} and 8.1 ± 0.7 µmol mg protein^{-1} min^{-1}, respectively (Supplementary Table S2). Neither isoform displayed co-operativity towards HCO_3^- binding, with Hill values close to 1.0 under all assay conditions (Supplementary Table S2).

The substitution of the conserved C_4 serine at residue 774 (780 in maize) with the conserved C_3 alanine (C_4-S774A) significantly increased the K_{HCO3} by 45% from 26.6 ± 1.7 µM to 38.6 ± 5.5 µM (Fig. 1). However, the C_4-S774A substitution had no effect on V_{Pmax} (Supplementary Table S2). The reverse substitution, C_3-A774S made in the C_3 PEPc, did not significantly change the K_{HCO3} (from 64.0 ± 2.4 µM to 61.5 ± 9.1 µM; Fig. 1) nor did it affect V_{Pmax} (Supplementary Table S2).

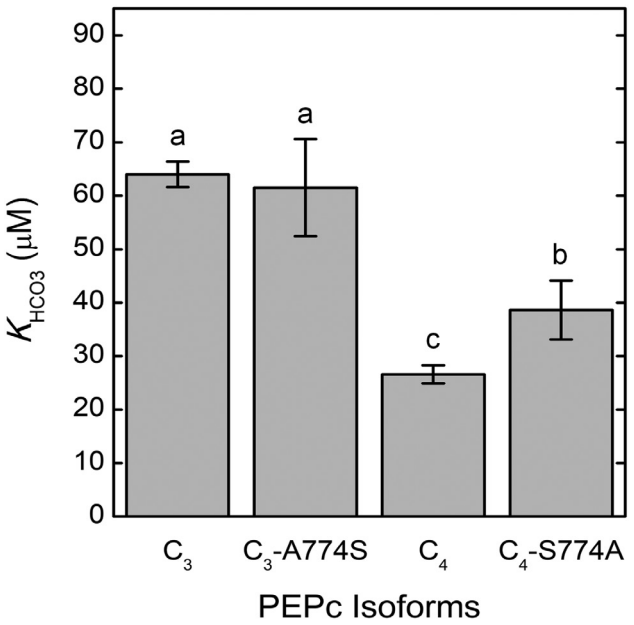


Fig. 1. The K_{HCO3} of the C_3, C_4, and chimeric PEPc isoforms. The K_{HCO3} values were obtained from the MIMS assayed in 100 mM HEPES-KOH buffer (pH 7.6) that contained 10 mM $MgCl_2$, 5 mM PEP, 50 µg ml^{-1} CA, 1 mM DTT, and 5 mM G6-P. Error bars represent the mean ±SD of four independent extractions from *E. coli* for each PEPc isoform. Significance was determined by one-way ANOVA and Tukey HSD post-hoc tests. Bars with different letters are significantly different ($P<0.05$).

The impact of G6-P and malate on K_{HCO3}

The V_{Pmax} did not change by omitting G6-P from the assay, regardless of the PEPc isoform (Supplementary Table S2). Additionally, the K_{HCO3} values of the PEPc isoforms were not significantly altered by the presence or absence of G6-P in the assay (Fig. 2).

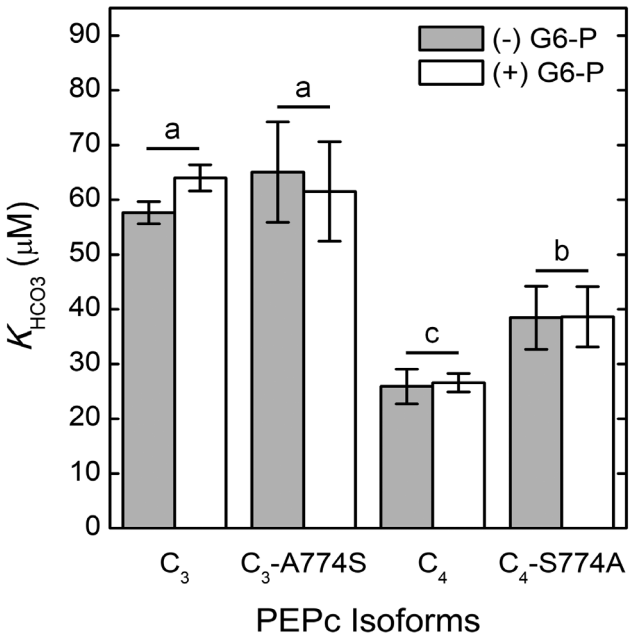


Fig. 2. The impact of G6-P on the K_{HCO3} of the different PEPc isoforms. The K_{HCO3} values of the different PEPc isoforms were obtained from MIMS PEPc assays where 5 mM G6-P was present (white bars) or absent (gray bars) in the assay buffer. White bars are data represented from Fig. 1. Error bars represent the mean ±SD of four independent extractions from *E. coli* for each PEPc isoform. A two-way ANOVA determined that G6-P had a non-significant effect on K_{HCO3} but there was a significant isoform effect, and a Tukey HSD post-hoc test was used to determined significance. PEPc isoforms with different letters are significantly different (P<0.005).

Under the current measurement conditions of pH 7.6, 5 mM PEP, and the absence of G6-P, the addition of 2.5 mM malate decreased the V_{Pmax} in the C_4, C_4-S774A chimeric, and the C_3 PEPc by 57.5, 24.4, and 6.8%, respectively (Supplementary Tables S2, S3). However, the K_{HCO3} values of the PEPc isoforms were not significantly altered by the presence of malate in the assay (Fig. 3A). HCO_3^- response curves in the absence of G6-P were not obtained for the C_3-A774S PEPc due to severe inhibition of the chimeric PEPc by malate (Supplementary Fig. S2). When 5 mM G6-P and 2.5 mM malate were both present in the PEPc assay, V_{Pmax} decreased in the C_4, C_4-S774A chimeric, C_3, and C_3-A774S chimeric PEPc by 44.4, 28.6, 2, and 14%, respectively (Supplementary Tables S2, S3). However, the K_{HCO3} values of the PEPc isoforms were not significantly changed with both G6-P and malate in the assay (Fig. 3B). Interestingly, decreasing the total PEP concentration in the assay from 5 mM to twice the reported K_{PEP} of the C_3 and C_4 isoforms (Bläsing *et al.*, 2002; Paulus *et al.*, 2013), 150 μM and 750 μM PEP, respectively, caused the C_3 PEPc to lose activity dramatically in the presence of malate, whereas the change in PEP concentration had a smaller effect on malate inhibition of C_4 PEPc activity (Fig. 4).

Effects of MIMS calibrations, assay conditions, and extraction sources on K_{HCO3}

At pH 7.6, the C_4 *F. trinervia* PEPc extracted from *E. coli* had a lower K_{HCO3} than desalted plant PEPc extracts from *F. trinervia*, 26.6 ± 1.7 μM and 35.2 ± 3.2 μM, respectively (Fig. 5A). Although not statistically significant, changing the pH of the assay buffer from 7.6 to 7.8 increased the K_{HCO3} of *S. viridis* PEPc by 21.3% from 30.0 ± 3.0 μM to 36.4 ± 5.3 μM (Fig. 5A, 5B). When using the Boyd *et al.* (2015) MIMS calibration method at pH 7.8, the *S. viridis* K_{HCO3} increased to 62.9 ± 8.7 μM (Fig. 5B).

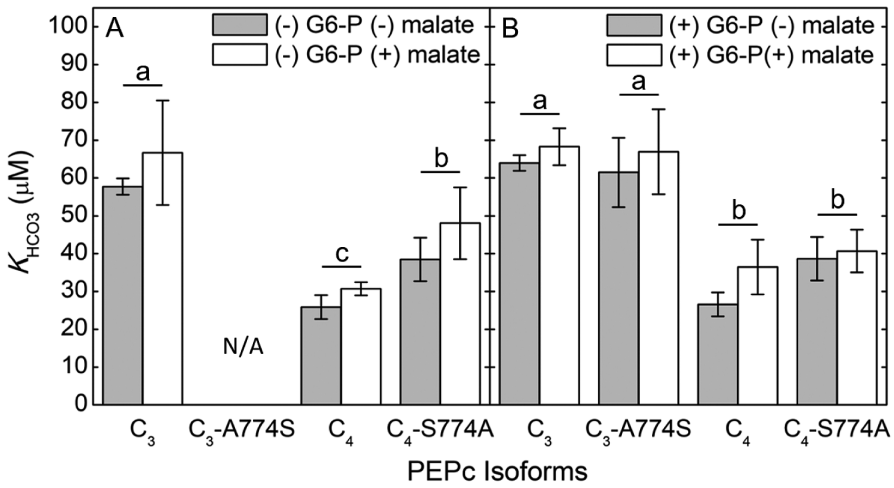


Fig. 3. The effect of 2.5 mM malate on the K_{HCO3} of different PEPc isoforms in the absence and presence of G6-P. (A) K_{HCO3} values of the different PEPc isoforms obtained from MIMS PEPc assays in the presence (white bars) or absence (gray bars) of 2.5 mM malate without G6-P. (B) The K_{HCO3} of the different PEPc isoforms with 5 mM G6-P, in the presence (white bars) or absence (gray bars) of 2.5 mM malate. Gray bars in both (A) and (B) represent data from previous figures. Error bars represent the mean ±SD of four independent extractions from *E. coli* for each PEPc isoform. A two-way ANOVA determined significant effects on K_{HCO3} by allosteric regulators and between different isoforms, but a Tukey HSD post-hoc test determined no significant allosteric effect on K_{HCO3} in both (A) and (B). A Tukey HSD post-hoc test was performed on the isoform effect, and different letters represent significant differences (P<0.005).

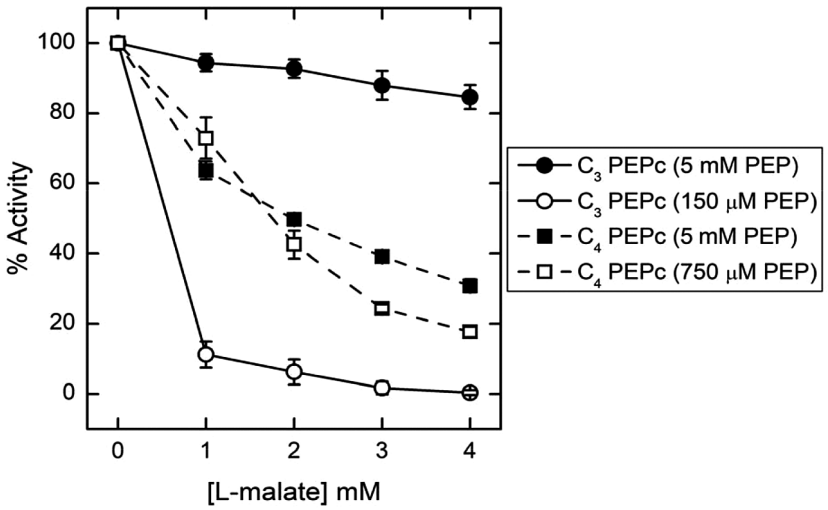


Fig. 4. Malate resistance of the C_3 PEPc is affected more by changing PEP concentrations than that of the C_4 PEPc. At 5 mM PEP (filled circles and squares), the C_3 PEPc (solid line) is more resistant to malate than the C_4 PEPc (dashed line). When the PEP concentration was dropped to twice the reported K_{PEP} for the C_3 and C_4 PEPc isoforms (open circles and squares), malate resistance of the C_3 PEPc dropped drastically compared with the malate resistance for the C_4 PEPc. Malate activity assays were performed in 100 mM HEPES-KOH (pH 7.6), 10 mM $MgCl_2$, 1 mM DTT, 50 μg ml^{-1} CA, 2.5 mM malate (pH 7.6), 1 mM $NaHCO_3$, and various PEP concentrations. Shapes and error bars represent the mean ±SD of four independent extractions from *E. coli* for both the C_3 and C_4 PEPc isoforms. A two-way repeated measures ANOVA (P<0.05) determined that there was a significant difference between the increased sensitivity to malate of the C_3 PEPc versus the C_4 PEPc when PEP concentration was decreased to 2×K_{PEP} for each isoform.

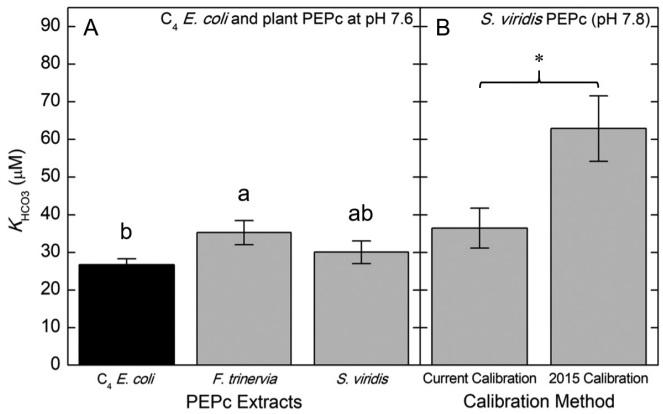


Fig. 5. The K_{HCO3} measured under different assay conditions for PEPc isoforms extracted from *F. trinervia*, *S. viridis*, and *E. coli*. (A) The K_{HCO3} values of the C_4 PEPc extracts from *E. coli* (black bar; value from Fig. 1) and desalted PEPc extracts from *F. trinervia* and *S. viridis* (gray bars) were obtained from the MIMS assayed in 100 mM HEPES-KOH buffer (pH 7.6) with 10 mM $MgCl_2$, 5 mM PEP, 50 μg ml^{-1} CA, 1 mM DTT, and 5 mM G6-P. Bars represent the mean ±SD of four independent PEPc extractions. Significance was determined by one-way ANOVA and Tukey HSD tests. Bars with different letters are significantly different (P<0.05). (B) *S. viridis* PEPc K_{HCO3} values measured from assays at pH 7.8 using either the current MIMS calibration or the Boyd *et al.* (2015) calibration. Significance between the K_{HCO3} of *S. viridis* PEPc assayed at (A) pH 7.6 and (B) 7.8 was determined by a Student's *t*-test (P=0.08). Significance between the K_{HCO3} of *S. viridis* PEPc assayed at pH 7.8 obtained by either the current calibration method or the Boyd *et al.* (2015) calibration method was determined by a Student's *t*-test (P<0.05).

Modeling the effect of different K_{HCO3} values on C_4 photosynthesis

The C_3 and C_4 PEPc K_{HCO3} values from Fig. 1 were input into the C_4 photosynthesis model from von Caemmerer (2000) to determine how differences in K_{HCO3} would impact modeled rates of C_4 photosynthesis. Varying K_{HCO3} with a constant V_{Pmax} significantly changed the modeled rates of C_4 photosynthesis under CO_2 conditions below 20 Pa. The lower K_{HCO3} of the C_4 PEPc resulted in higher modeled rates of C_4 photosynthesis at these low mesophyll CO_2 concentrations (C_m; Fig. 6). However, the difference between the C_3 and C_4 K_{HCO3} modeled no differences in net CO_2 assimilation above ~20 Pa C_m (Fig. 6).

Discussion

Kinetic changes during the evolution of the C_4 PEPc

We and others (Jacobs *et al.*, 2008; Gowik and Westhoff, 2011) have hypothesized that there was a strong selective pressure to reduce the K_{HCO3} of the C_4 PEPc isoform. Additionally, previous studies have reported that changing the PEPc amino acid residue 774 in *Flaveria* spp. (780 in maize) influences K_{PEP} and its allosteric regulation (Engelmann *et al.*, 2002; Endo *et al.*, 2008). Therefore, the aim of this research was to test the hypotheses that the K_{HCO3} of the C_4 PEPc isoform from *F. trinervia* would be lower than the K_{HCO3} of the C_3 PEPc isoform from *F. pringlei* and that changes to residue 774 will impact K_{HCO3} and its allosteric regulation. Residue 774 was chosen because others have shown the C_4 *F. trinervia* S774A substitution reduces K_{PEP} (Bläsing *et al.*, 2000; Endo *et al.*, 2008). Furthermore, residue 774 is near both the PEP- and HCO_3^--binding sites, and may also influence K_{HCO3}. We have analyzed the influence of this residue on K_{HCO3} and showed that the C_4-S774A chimeric PEPc had a significantly higher K_{HCO3} compared with the C_4 PEPc (Fig. 1). This fits with previous data that suggest that K_{PEP} and K_{HCO3} are inversely linked through specific amino acid residues near the two binding sites. For example, the K829G substitution in the *F. trinervia* C_4 PEPc resulted in a small decrease in K_{HCO3} and a simultaneous increase to K_{PEP} (Gao and Woo, 1996). Alternatively, swapping Lys600 with either an arginine or threonine in *F. trinervia* led

to increases in both K_{PEP} and K_{HCO3}, but this residue is one of the four conserved amino acids comprising the HCO_3^--binding site (Gao and Woo, 1995; Kai *et al.*, 2003).

The chimeric C_3 PEPc of *F. pringlei*, C_3-A774S, had a minimal effect on K_{HCO3} (Fig. 1). This same amino acid substitution was also shown not to influence the K_{PEP} of the C_3 PEPc with G6-P present in the assay. However, in the absence of G6-P, the same A774S substitution did increase K_{PEP} (Bläsing *et al.*, 2000). Taken together, these results support the analysis that multiple amino acid residues, in addition to S774 (S780 in maize), influence PEPc kinetics. Indeed, swapping amino acid residues 296–437 from the C_4 enzyme into the C_3-A774S chimeric PEPc increased the C_3 K_{PEP} even closer to the established C_4 K_{PEP} value (Engelmann *et al.*, 2002). However, further research is needed to understand how changes in PEPc amino acid composition influence K_{HCO3}, particularly how specific amino acid changes influence the impact that allosteric regulators such as G6-P and malate have on K_{HCO3}.

The influence of G6-P and malate on K_{HCO3}

PEPc is regulated by post-translational modifications (PTMs) and interactions with allosteric effectors. Previous studies showed that glycine and G6-P activate PEPc (Svensson *et al.*, 1997; Westhoff *et al.*, 1997; Endo *et al.*, 2008) while the end-products, aspartic acid and malate, inhibit PEPc (Huber and Edwards, 1975). Additionally, previous studies have shown that the PEP-binding sites of the C_4 PEPc tetramer display positive co-operativity for K_{PEP}, which can be altered by the binding of G6-P and malate to PEPc (Wedding *et al.*, 1990; Bläsing *et al.*, 2002; Rosnow *et al.*, 2015). We show that neither G6-P nor malate appears to impact K_{HCO3} and the co-operativity of HCO_3^- binding to the extent that they influence K_{PEP} and co-operative PEP binding (Figs 2, 3; Supplementary Tables S2, S3). Using the crystal structure (4BXC) deposited by Schlieper *et al.* (2014), the HCO_3^--binding site is further from the G6-P and aspartic acid/malate allosteric binding sites than the PEP-binding site is from the allosteric sites, so any structural changes to PEPc caused by allosteric binding may affect the PEP-binding site more than the HCO_3^--binding site. Additionally, the S774A and A774S substitutions did not influence the allosteric regulation of PEPc to the extent that the R884G and G884R substitutions affected malate sensitivity of the *F. pringlei* and *F. trinervia* PEPc isoforms, respectively (Paulus *et al.*, 2013). This discrepancy may be due to residue 884 being closer to the residues of the aspartate/malate-binding sites compared with residue 774, whereas residue 774 is closer to the PEP- and HCO_3^--binding sites (Kai *et al.*, 2003; Paulus *et al.*, 2013).

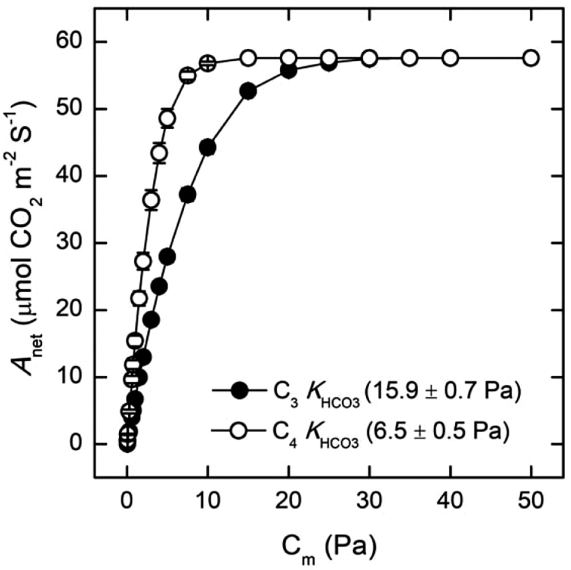


Fig. 6. Modeled rates of C_4 photosynthesis with C_3 and C_4 K_{HCO3}. The K_{HCO3} values for the C_3 PEPc (filled circles) and C_4 PEPc (open circles) were input into the C_4 photosynthesis model from von Caemmerer (2000) to determine the modeled rate of CO_2 assimilation (A_{net}) at various mesophyll CO_2 concentrations (C_m). Symbols represent means ±SD of four independent K_{HCO3} values presented in Fig. 1 input into the model, where all other variables in the C_4 model were held constant. The maximal rates of PEP regeneration (V_{pr}), Rubisco carboxylation (V_{Cmax}), and maximum PEPc carboxylation per unit leaf area [$V_{Pmax(plant)}$] were set to 80, 60, and 120 µmol m^{-2} s^{-1}, respectively (von Caemmerer, 2000), and all other values are presented in Supplementgary Table S1. A pK_a of 6.12 and assumed a mesophyll cytosol pH of 7.2 were used to convert µM HCO_3^- to µM CO_2. Pa CO_2 was obtained by using Henry's constant for CO_2 (0.034 mol l^{-1} atm^{-1}) and assumed standard pressure (101 325 Pa atm^{-1}).

Another possibility is that PEP binds before HCO_3^- (Janc *et al.*, 1992), potentially conferring the primary allosteric regulation of PEPc to the binding of PEP. Alternatively, under our assay conditions, the high PEP concentration may have reduced the impact G6-P and malate had on K_{HCO3}. For example, G6-P has a greater activating effect on PEPc under limiting PEP concentrations at 0.5 mM (Gupta *et al.*, 1994). In addition, multiple studies suggest that there is a regulatory PEP-binding site different from the PEPc active site (Rustin *et al.*, 1988; Rodríguez-Sotres and Muñoz-Clares, 1990; Mújica-Jiménez *et al.*, 1998; Yuan *et al.*, 2006), and it is possible this regulatory PEP site may not be saturated under low PEP concentrations. Saturating this regulatory PEP-binding site might supersede G6-P activation and overcome malate inhibition of PEPc (Huber and Edwards, 1975). The assay conditions used in this study contained saturating (5 mM) levels of PEP, which were well above the K_{PEP} of both PEPc isoforms, since limiting PEP would complicate the response to changes in HCO_3^- concentrations. The C_3 PEPc was more resistant to malate inhibition than the C_4 PEPc under these saturating PEP conditions, which is in contrast to previous reports (Bläsing *et al.*, 2002; Paulus *et al.*, 2013). However, we found that the C_3 PEPc was more sensitive to malate than the C_4 PEPc when the PEP concentration in the assay was reduced to 2×K_{PEP} (Fig. 4). This suggests that the PEP regulatory site for the C_4 PEPc may be less sensitive than the C_3 PEPc to changes in free PEP availability. Alternatively, the C_4 PEP regulatory site may not have as much influence on malate tolerance as the C_3 PEP regulatory site under the current assay conditions.

We were unable to obtain kinetic data for the C_3-A774S chimeric PEPc due to drastic inhibition of the enzyme by malate when G6-P was absent from the assay (Supplementary Fig. S2). This result was unexpected since the addition of 2.5 mM malate had a small effect on the activity of the C_3 PEPc (Supplementary Tables S2, S3). However, since PEP and

malate interact differently with the C_3 and C_4 PEPc isoforms, it is possible that the A774S substitution in the C_3 PEPc modified these interactions to allow potent inhibition of the C_3-A774S chimeric PEPc. Further analysis is needed to test the extent of malate inhibition on the C_3-A774S PEPc and other chimeric PEPc isoforms under various assay conditions. It is worth noting that malate has a stronger inhibitory effect on PEPc at pH 7.0 than at pH 8.0 (Huber and Edwards, 1975; Gupta *et al.*, 1994). As discussed below, pH and other assay conditions used to measure PEPc activity can influence the absolute values of the kinetic parameters.

Assay conditions, extraction method, and source can affect PEPc kinetics

MIMS can directly measure dissolved CO_2 even at very low C_i concentrations below the K_{HCO3} of PEPc (Beckmann *et al.*, 2009; Cousins *et al.*, 2010). Previously, Boyd *et al.* (2015) reported a MIMS-measured K_{HCO3} value of 62.8 μM for the *S. viridis* C_4 PEPc which is higher than our MIMS-measured K_{HCO3} value of 26.6 μM for the *F. trinervia* C_4 PEPc extracted from *E. coli*. This difference in K_{HCO3} between the *S. viridis* and *F. trinervia* C_4 PEPc may be due to any combination of species differences in enzyme kinetics, enzyme purity, pH of the assay, and MIMS calibrations. Plant PEPc extracted from *F. trinervia*, a dicot in the Asteraceae family, and *S. viridis*, a monocot in the Poaceae family, had similar K_{HCO3} values at pH 7.6 (Fig. 5A). Bauwe (1986) also reported similar K_{HCO3} values for different C_4 PEPc isoforms extracted from multiple grasses and *Glomphrena globosa*, a dicot from the Amaranthaceae family.

The *F. trinervia* C_4 PEPc partially purified from *E. coli* was reported to be unphosphorylated at the N-terminal serine residue (Svensson *et al.*, 1997) and had a significantly lower K_{HCO3} than the desalted plant PEPc extracts taken from *F. trinervia* leaves during the day (Fig. 5). This suggests that potential differences in post-translational modifications might influence the kinetic properties of PEPc. Parvathi *et al.* (2000) observed a decrease in K_{HCO3} as PEPc changed from the unphosphorylated to the phosphorylated state, and that PEPc extracts from illuminated leaves had lower K_{HCO3} values than PEPc extracted in the dark. In the current study, the phosphorylation status of the PEPc extracts was not tested, so it cannot be confirmed that the difference in K_{HCO3} between the plant and *E. coli* extracts is due to changes in PTMs. Alternatively, Bauwe (1986) observed that unpurified C_4 PEPc had higher K_{HCO3} values than purified C_4 PEPc extracts. It is possible that the impurity of our desalted plant PEPc extracts from *F. trinervia* contributed to the increased K_{HCO3} relative to the C_4 PEPc purified from *E. coli*. The potential differences in PTMs and enzyme purity do not completely explain why the K_{HCO3} for the *S. viridis* PEPc reported here and by Boyd *et al.* (2015) differ; however, this discrepancy in K_{HCO3} can be explained by differences in assay conditions and MIMS calibrations.

Raising the pH of the PEPc assay from 7.6 to 7.8, the pH used by Boyd *et al.* (2015), increased the *S. viridis* PEPc K_{HCO3} by ~21% (Fig. 5A, B). In addition to the pH of the assay buffer, the MIMS calibration method can alter the measured K_{HCO3}. This is because two MIMS calibrations are required to convert a voltage signal of mass 44 to a micromolar concentration of CO_2 and to determine the HCO_3^- concentration in the reaction cuvette. Since the development of a novel MIMS technique to measure K_{HCO3} of PEPc (Boyd *et al.*, 2015), we have improved the MIMS calibration method to obtain more accurate K_{HCO3} values to analyze kinetic differences between PEPc isoforms. The calibration method presented here differed from that of Boyd *et al.* (2015) because all reaction components except the enzyme extract were included in the calibration. This would account for slight pH changes to the assay when adding DTT, G6-P, or PEP, which is important for determining the CO_2:HCO_3^- ratio. If there is a slight reduction in pH from adding assay components that is not accounted for during the calibrations, then the CO_2:HCO_3^- ratio can be slightly overestimated, leading to higher estimations of K_{HCO3}. Using the calibration method and pH of 7.8 from Boyd *et al.* (2015), the K_{HCO3} values reported here (62.9 ± 8.7 μM) and by Boyd *et al.* (2015) (62.8 ± 5.0 μM) were nearly identical (Fig. 5B), suggesting that assay conditions such as pH and differences in MIMS calibration methods can affect the estimated K_{HCO3}. These findings also highlight the important consideration of how well *in vitro* assay conditions reflect the *in vivo* conditions where PEPc operates. So far, *in vivo* PEPc kinetics can only be obtained by models using gas exchange (von Caemmerer, 2000). Further research is needed to compare *in vitro* and *in vivo* PEPc kinetics, since accurate PEPc kinetics are needed to model C_4 photosynthesis.

K_{HCO3} affects modeled rates of C_4 photosynthesis

The C_4 photosynthesis model developed by von Caemmerer (2000) was used to test if differences in K_{HCO3} between the C_3 and C_4 PEPc isoforms were enough to influence rates of net CO_2 assimilation during C_4 photosynthesis. The C_4 model predicts that a lower K_{HCO3} may not affect photosynthetic rates under high CO_2 partial pressures (Fig. 6). This is expected since C_4 photosynthesis rates are typically not limited by PEPc under these conditions (von Caemmerer, 2000). However, a large K_{HCO3} may limit rates of C_4 photosynthesis under low CO_2 partial pressures (Fig. 6), for example when reduced stomatal conductance limits CO_2 movement into the leaf. Flux control analysis found that PEPc has substantial control of C_4 photosynthesis under low CO_2 partial pressures (Dever *et al.*, 1997; Bailey *et al.*, 2000). Therefore, there is likely to be strong selective pressure to increase PEPc affinity for HCO_3^- in C_4 plants to increase the amount of C_i entering C_4 photosynthesis. Our results, combined with those of others (Bläsing *et al.*, 2000; Engelmann *et al.*, 2002; Endo *et al.*, 2008), show that as C_4 K_{HCO3} dropped, there was a concurrent increase in C_4 K_{PEP}. Due to the higher PEP levels observed in leaves of C_4 plants compared with C_3 plants (Leegood and von Caemmerer, 1994), it can be argued that there was stronger selective pressure to increase PEPc affinity for HCO_3^- than to maintain high affinities for PEP since an increase in K_{PEP} may not negatively impact C_4 photosynthesis rates to the extent that changes in K_{HCO3} can under lower CO_2 partial pressures (Fig. 6).

Conclusion

The direct comparison of closely related C_3 and C_4 PEPc isoforms from *Flaveria* demonstrates that the photosynthetic C_4 PEPc isoform has a significantly higher affinity for HCO_3^- than its closely

related C_3 PEPc isoform. This reduced K_{HCO3} impacts net CO_2 assimilation rates, particularly at low CO_2 availability, suggesting selective pressure to reduce the C_4 K_{HCO3} to optimize inorganic carbon flux through C_4 photosynthesis. Alternatively, the increase in K_{PEP} can be seen as strengthening the diurnal regulation of C_4 PEPc but residue S774 appears to link K_{HCO3} and K_{PEP}, indicating that the increase in K_{PEP} could be a negative consequence of reducing K_{HCO3}. Testing different plant species will provide new insights into which amino acids control K_{HCO3} and provide a better understanding of the structure and function relationship of the enzyme. Obtaining a better understanding of what controls K_{HCO3} will also lead to enhancing C_4 photosynthesis, particularly at low CO_2 partial pressures when stomata are partially closed. This raises interesting questions of whether there is a range in K_{HCO3} across the diverse lineages of C_4 plants and finding relationships between certain amino acid residues and ranges of K_{HCO3} values can be beneficial for promoting strategies to optimize C_4 photosynthesis in crop species for drought conditions.

Supplementary data

Supplementary data are available at *JXB* online.

Table S1. Variable descriptions and values used to model C_4 photosynthesis.

Table S2. Kinetic properties of PEPc isoforms from *F. trinervia* and *F. pringlei*.

Table S3. Kinetic properties of PEPc isoforms in the presence of 2.5 mM malate.

Fig. S1. Representative MIMS responses of the C_3 and C_4 PEPc activities with changing HCO_3^- concentrations.

Fig. S2. HCO_3^- response curves for the C_3, C_3-A774S, C_4, and C_4-S774A PEPc isoforms in the presence of 2.5 mM malate.

Acknowledgements

This work was supported by the Division of Chemical Sciences, Geosciences, and Biosciences, Office of Basic Energy Sciences, Department of Energy (grant no. DE-SC0001685) and the National Science Foundation (Major Research Instrumentation grant no. 0923562). The authors declare no conflicts of interest. Thanks to Professor Peter Westhoff for donating the *E. coli* strain and plasmids used in this work, Dr Udo Gowik for discussions on PEPc purification and PEP kinetics, and Dr Ryan Boyd for discussions on MIMS calibrations, PEPc assays, and MIMS data analysis.

References

Bailey KJ, Battistelli A, Dever LV, Lea PJ, Leegood RC. 2000. Control of C_4 photosynthesis: effects of reduced activities of phosphoenolpyruvate carboxylase on CO_2 assimilation in *Amaranthus edulis* L. Journal of Experimental Botany **51 Spec No,** 339–346.

Bauwe H. 1986. An efficient method for the determination of K m values for HCO_3^- of phosphoenolpyruvate carboxylase. Planta **169,** 356–360.

Beckmann K, Messinger J, Badger MR, Wydrzynski T, Hillier W. 2009. On-line mass spectrometry: membrane inlet sampling. Photosynthesis Research **102,** 511–522.

Bläsing OE, Ernst K, Streubel M, Westhoff P, Svensson P. 2002. The non-photosynthetic phosphoenolpyruvate carboxylases of the C_4 dicot *Flaveria trinervia*—implications for the evolution of C_4 photosynthesis. Planta **215,** 448–456.

Bläsing OE, Westhoff P, Svensson P. 2000. Evolution of C_4 phosphoenolpyruvate carboxylase in *Flaveria*, a conserved serine residue in the carboxyl-terminal part of the enzyme is a major determinant for C_4-specific characteristics. Journal of Biological Chemistry **275,** 27917–27923.

Boyd RA, Gandin A, Cousins AB. 2015. Temperature responses of C_4 photosynthesis: biochemical analysis of Rubisco, phosphoenolpyruvate carboxylase, and carbonic anhydrase in *Setaria viridis*. Plant Physiology **169,** 1850–1861.

Bradford MM. 1976. A rapid and sensitive method for the quantitation of microgram quantities of protein utilizing the principle of protein–dye binding. Analytical Biochemistry **72,** 248–254.

Britto DT, Kronzucker HJ. 2005. Nitrogen acquisition, PEP carboxylase, and cellular pH homeostasis: new views on old paradigms. Plant, Cell & Environment **28,** 1396–1409.

Budde RJ, Chollet R. 1986. In vitro phosphorylation of maize leaf phosphoenolpyruvate carboxylase. Plant Physiology **82,** 1107–1114.

Christin PA, Besnard G. 2009. Two independent C_4 origins in Aristidoideae (Poaceae) revealed by the recruitment of distinct phosphoenolpyruvate carboxylase genes. American Journal of Botany **96,** 2234–2239.

Christin PA, Salamin N, Savolainen V, Duvall MR, Besnard G. 2007. C_4 photosynthesis evolved in grasses via parallel adaptive genetic changes. Current Biology: CB **17,** 1241–1247.

Cousins AB, Baroli I, Badger MR, Ivakov A, Lea PJ, Leegood RC, von Caemmerer S. 2007. The role of phosphoenolpyruvate carboxylase during C_4 photosynthetic isotope exchange and stomatal conductance. Plant Physiology **145,** 1006–1017.

Cousins AB, Ghannoum O, von Caemmerer S, Badger MR. 2010. Simultaneous determination of Rubisco carboxylase and oxygenase kinetic parameters in *Triticum aestivum* and *Zea mays* using membrane inlet mass spectrometry. Plant, Cell & Environment **33,** 444–452.

Davies DD. 1986. The fine control of cytosolic pH. Physiologia Plantarum **67,** 702–706.

Dever LV, Bailey KJ, Leegood RC, Lea PJ. 1997. Control of photosynthesis in *Amaranthus edulis* mutants with reduced amounts of PEP carboxylase. Functional Plant Biology **24,** 469–476.

Dong LY, Masuda T, Kawamura T, Hata S, Izui K. 1998. Cloning, expression, and characterization of a root-form phosphoenolpyruvate carboxylase from *Zea mays*: comparison with the C_4-form enzyme. Plant & Cell Physiology **39,** 865–873.

Endo T, Mihara Y, Furumoto T, Matsumura H, Kai Y, Izui K. 2008. Maize C_4-form phosphoenolpyruvate carboxylase engineered to be functional in C_3 plants: mutations for diminished sensitivity to feedback inhibitors and for increased substrate affinity. Journal of Experimental Botany **59,** 1811–1818.

Engelmann S, Bläsing OE, Westhoff P, Svensson P. 2002. Serine 774 and amino acids 296 to 437 comprise the major C_4 determinants of the C_4 phosphoenolpyruvate carboxylase of *Flaveria trinervia*. FEBS Letters **524,** 11–14.

Gao Y, Woo KC. 1995. Site-directed mutagenesis of Lys600 in phosphoenolpyruvate carboxylase of *Flaveria trinervia*: its roles in catalytic and regulatory functions. FEBS Letters **375,** 95–98.

Gao Y, Woo KC. 1996. Site-directed mutagenesis of *Flaveria trinervia* phosphoenolpyruvate carboxylase: Arg450 and Arg767 are essential for catalytic activity and Lys829 affects substrate binding. FEBS Letters **392,** 285–288.

Gowik U, Burscheidt J, Akyildiz M, Schlue U, Koczor M, Streubel M, Westhoff P. 2004. *cis*-Regulatory elements for mesophyll-specific gene expression in the C_4 plant *Flaveria trinervia*, the promoter of the C_4 phosphoenolpyruvate carboxylase gene. The Plant Cell **16,** 1077–1090.

Gowik U, Engelmann S, Bläsing OE, Raghavendra AS, Westhoff P. 2006. Evolution of C_4 phosphoenolpyruvate carboxylase in the genus *Alternanthera*: gene families and the enzymatic characteristics of the C_4 isozyme and its orthologues in C_3 and C_3/C_4 *Alternantheras*. Planta **223,** 359–368.

Gowik U, Westhoff P. 2011. C_4-phosphoenolpyruvate carboxylase. In: Raghavendra AS, Sage RF, eds. C_4 photosynthesis and related CO_2 concentrating mechanisms. Dordrecht, The Netherlands: Springer, 257–275.

Gupta SK, Ku MS, Lin JH, Zhang D, Edwards GE. 1994. Light/dark modulation of phospho*enol*pyruvate carboxylase in C_3 and C_4 species. Photosynthesis Research **42,** 133–143.

Hatch MD. 1987. C_4 photosynthesis: a unique blend of modified biochemistry, anatomy and ultrastructure. Biochimica et Biophysica Acta **895,** 81–106.

Hatch MD, Kagawa T, Craig S. 1975. Subdivision of C_4-pathway species based on differing C_4 acid decarboxylating systems and ultrastructural features. Functional Plant Biology **2,** 111–128.

Hermans J, Westhoff P. 1992. Homologous genes for the C_4 isoform of phosphoenolpyruvate carboxylase in a C_3 and a C_4 *Flaveria* species. Molecular & General Genetics **234,** 275–284.

Huber SC, Edwards GE. 1975. Inhibition of phosphoenolpyruvate carboxylase from C_4 plants by malate and aspartate. Canadian Journal of Botany **53,** 1925–1933.

Jacobs B, Engelmann S, Westhoff P, Gowik U. 2008. Evolution of C_4 phosphoenolpyruvate carboxylase in *Flaveria*: determinants for high tolerance towards the inhibitor L-malate. Plant, Cell & Environment **31,** 793–803.

Janc JW, O'Leary MH, Cleland WW. 1992. A kinetic investigation of phosphoenolpyruvate carboxylase from *Zea mays*. Biochemistry **31,** 6421–6426.

Kai Y, Matsumura H, Izui K. 2003. Phosphoenolpyruvate carboxylase: three-dimensional structure and molecular mechanisms. Archives of Biochemistry and Biophysics **414,** 170–179.

Lara MV, Chuong SD, Akhani H, Andreo CS, Edwards GE. 2006. Species having C_4 single-cell-type photosynthesis in the Chenopodiaceae family evolved a photosynthetic phosphoenolpyruvate carboxylase like that of Kranz-type C_4 species. Plant Physiology **142,** 673–684.

Leegood RC, von Caemmerer S. 1994. Regulation of photosynthetic carbon assimilation in leaves of C_3–C_4 intermediate species of *Moricandia* and *Flaveria*. Planta **192,** 232–238.

Mújica-Jiménez C, Castellanos-Martínez A, Muñoz-Clares RA. 1998. Studies of the allosteric properties of maize leaf phosphoenolpyruvate carboxylase with the phosphoenolpyruvate analog phosphomycin as activator. Biochimica et Biophysica Acta **1386,** 132–144.

O'Leary B, Park J, Plaxton WC. 2011. The remarkable diversity of plant PEPC (phosphoenolpyruvate carboxylase): recent insights into the physiological functions and post-translational controls of non-photosynthetic PEPCs. Biochemical Journal **436,** 15–34.

Parvathi K, Bhagwat AS, Ueno Y, Izui K, Raghavendra AS. 2000. Illumination increases the affinity of phosphoenolpyruvate carboxylase to bicarbonate in leaves of a C_4 plant, *Amaranthus hypochondriacus*. Plant & Cell Physiology **41,** 905–910.

Parvathi K, Raghavendra AS. 1997. Both rubisco and phosphoenolpyruvate carboxylase are beneficial for stomatal function in epidermal strips of *Commelina benghalensis*. Plant Science **124,** 153–157.

Paulus JK, Schlieper D, Groth G. 2013. Greater efficiency of photosynthetic carbon fixation due to single amino-acid substitution. Nature Communications **4,** 1518.

Plaxton WC, Podestá FE. 2006. The functional organization and control of plant respiration. Critical Reviews in Plant Sciences **25,** 159–198.

Poetsch W, Hermans J, Westhoff P. 1991. Multiple cDNAs of phosphoenolpyruvate carboxylase in the C_4 dicot *Flaveria trinervia*. FEBS Letters **292,** 133–136.

Rademacher T, Häusler RE, Hirsch HJ, Zhang L, Lipka V, Weier D, Kreuzaler F, Peterhänsel C. 2002. An engineered phosphoenolpyruvate carboxylase redirects carbon and nitrogen flow in transgenic potato plants. The Plant Journal **32,** 25–39.

Rodríguez-Sotres R, Muñoz-Clares RA. 1990. Kinetic evidence of the existence of a regulatory phosphoenolpyruvate binding site in maize leaf phosphoenolpyruvate carboxylase. Archives of Biochemistry and Biophysics **276,** 180–190.

Rosnow JJ, Edwards GE, Roalson EH. 2014. Positive selection of Kranz and non-Kranz C_4 phosphoenolpyruvate carboxylase amino acids in Suaedoideae (Chenopodiaceae). Journal of Experimental Botany **65,** 3595–3607.

Rosnow JJ, Evans MA, Kapralov MV, Cousins AB, Edwards GE, Roalson EH. 2015. Kranz and single-cell forms of C_4 plants in the subfamily Suaedoideae show kinetic C_4 convergence for PEPC and Rubisco with divergent amino acid substitutions. Journal of Experimental Botany **66,** 7347–7358.

RStudio Team. 2016. RStudio: integrated development for R. Boston, MA: RStudio, Inc. http://www.rstudio.com/.

Rustin P, Meyer CR, Wedding RT. 1988. Identification of substrate and effector binding sites of phosphoenolpyruvate carboxylase from *Crassula argentea*. A possible role of phosphoenolpyruvate as substrate and activator. Journal of Biological Chemistry **263,** 17611–17614.

Sabe H, Miwa T, Kodaki T, Izui K, Hiraga S, Katsuki H. 1984. Molecular cloning of the phosphoenolpyruvate carboxylase gene, *ppc*, of *Escherichia coli*. Gene **31,** 279–283.

Sangwan RS, Singh N, Plaxton WC. 1992. Phosphoenolpyruvate carboxylase activity and concentration in the endosperm of developing and germinating castor oil seeds. Plant Physiology **99,** 445–449.

Schäffner AR, Sheen J. 1992. Maize C_4 photosynthesis involves differential regulation of phosphoenolpyruvate carboxylase genes. The Plant Journal **2,** 221–232.

Schlieper D, Förster K, Paulus JK, Groth G. 2014. Resolving the activation site of positive regulators in plant phosphoenolpyruvate carboxylase. Molecular Plant **7,** 437–440.

Svensson P, Bläsing OE, Westhoff P. 1997. Evolution of the enzymatic characteristics of C_4 phospho*enol*pyruvate carboxylase—a comparison of the orthologous *PPCA* phospho*enol*pyruvate carboxylases of *Flaveria trinervia* (C_4) and *Flaveria pringlei* (C_3). European Journal of Biochemistry **246,** 452–460.

Tholen D, Zhu XG. 2011. The mechanistic basis of internal conductance: a theoretical analysis of mesophyll cell photosynthesis and CO_2 diffusion. Plant Physiology **156,** 90–105.

Ubierna N, Sun W, Kramer DM, Cousins AB. 2013. The efficiency of C_4 photosynthesis under low light conditions in *Zea mays*, *Miscanthus* × *giganteus* and *Flaveria bidentis*. Plant, Cell & Environment **36,** 365–381.

von Caemmerer S. 2000. Biochemical models of leaf photosynthesis. Collingwood VIC, Australia: CSIRO Publishing.

von Caemmerer S, Evans JR, Hudson GS, Andrews TJ. 1994. The kinetics of ribulose-1,5-bisphosphate carboxylase/oxygenase in vivo inferred from measurements of photosynthesis in leaves of transgenic tobacco. Planta **195,** 88–97.

von Caemmerer S, Furbank RT. 2003. The C_4 pathway: an efficient CO_2 pump. Photosynthesis Research **77,** 191–207.

Wedding RT, Black MK, Meyer CR. 1990. Inhibition of phosphoenolpyruvate carboxylase by malate. Plant Physiology **92,** 456–461.

Westhoff P, Gowik U. 2004. Evolution of C_4 phosphoenolpyruvate carboxylase. Genes and proteins: a case study with the genus *Flaveria*. Annals of Botany **93,** 13–23.

Westhoff P, Svensson P, Ernst K, Bläsing O, Burscheidt J, Stockhaus J. 1997. Molecular evolution of C_4 phosphoenolpyruvate carboxylase in the genus *Flaveria*. Functional Plant Biology **24,** 429–436.

Yuan J, Sayegh J, Mendez J, Sward L, Sanchez N, Sanchez S, Waldrop G, Grover S. 2006. The regulatory role of residues 226–232 in phosphoenolpyruvate carboxylase from maize. Photosynthesis Research **88,** 73–81.